

Tribology of Co-sputtered Nanocomposite Au/MoS₂ Solid Lubricant Films Over a Wide Contact Stress Range

15 January 2005

Prepared by

J. R. LINCE
Space Materials Laboratory
Laboratory Operations

Prepared for

SPACE AND MISSILE SYSTEMS CENTER
AIR FORCE SPACE COMMAND
2430 E. El Segundo Boulevard
Los Angeles Air Force Base, CA 90245

Engineering and Technology Group

20050314 122




El Segundo, California

APPROVED FOR PUBLIC RELEASE;
DISTRIBUTION UNLIMITED

This report was submitted by The Aerospace Corporation, El Segundo, CA 90245-4691, under Contract No. FA8802-04-C-0001 with the Space and Missile Systems Center, 2430 E. El Segundo Blvd., Los Angeles Air Force Base, CA 90245. It was reviewed and approved for The Aerospace Corporation by P. D. Fleischauer, Principal Director, Space Materials Laboratory. Michael Zambrana was the project officer for the Mission-Oriented Investigation and Experimentation (MOIE) program.

This report has been reviewed by the Public Affairs Office (PAS) and is releasable to the National Technical Information Service (NTIS). At NTIS, it will be available to the general public, including foreign nationals.

This technical report has been reviewed and is approved for publication. Publication of this report does not constitute Air Force approval of the report's findings or conclusions. It is published only for the exchange and stimulation of ideas.



Michael Zambrana
SMC/AXE

REPORT DOCUMENTATION PAGE				Form Approved OMB No. 0704-0188	
Public reporting burden for this collection of information is estimated to average 1 hour per response, including the time for reviewing instructions, searching existing data sources, gathering and maintaining the data needed, and completing and reviewing this collection of information. Send comments regarding this burden estimate or any other aspect of this collection of information, including suggestions for reducing this burden to Department of Defense, Washington Headquarters Services, Directorate for Information Operations and Reports (0704-0188), 1215 Jefferson Davis Highway, Suite 1204, Arlington, VA 22202-4302. Respondents should be aware that notwithstanding any other provision of law, no person shall be subject to any penalty for failing to comply with a collection of information if it does not display a currently valid OMB control number. PLEASE DO NOT RETURN YOUR FORM TO THE ABOVE ADDRESS.					
1. REPORT DATE (DD-MM-YYYY) 15-01-2005		2. REPORT TYPE		3. DATES COVERED (From - To)	
4. TITLE AND SUBTITLE Tribology of Co-sputtered Nanocomposite Au/ MoS ₂ Solid Lubricant Films Over a Wide Contact Stress Range				5a. CONTRACT NUMBER FA8802-04-C-0001	
				5b. GRANT NUMBER	
				5c. PROGRAM ELEMENT NUMBER	
6. AUTHOR(S) J. R. Lince				5d. PROJECT NUMBER	
				5e. TASK NUMBER	
				5f. WORK UNIT NUMBER	
7. PERFORMING ORGANIZATION NAME(S) AND ADDRESS(ES) The Aerospace Corporation Laboratory Operations El Segundo, CA 90245-4691				8. PERFORMING ORGANIZATION REPORT NUMBER TR-2005(8565)-1	
9. SPONSORING / MONITORING AGENCY NAME(S) AND ADDRESS(ES) Space and Missile Systems Center Air Force Space Command 2450 E. El Segundo Blvd. Los Angeles Air Force Base, CA 90245				10. SPONSOR/MONITOR'S ACRONYM(S) SMC	
				11. SPONSOR/MONITOR'S REPORT NUMBER(S) SMC-TR-05-12	
12. DISTRIBUTION/AVAILABILITY STATEMENT Approved for public release; distribution unlimited.					
13. SUPPLEMENTARY NOTES					
14. ABSTRACT Slip-ring assemblies for spacecraft, and other sliding electrical contacts, require low friction and wear, as well as low electrical resistance and noise. Most current slip-ring technologies (both solid- and liquid-lubricated) are over forty years old, and their robustness is often less than satisfactory. Newer technologies have been developed, but have also shown limitations in spacecraft applications. We are investigating alternate material technologies to address these issues, concentrating on sputter-deposition of metals (e.g., gold) containing solid lubricants (e.g., MoS ₂) to form electrically conductive, lubricious nanocomposite films. In the present study, we investigated the friction and endurance of co-sputtered Au/MoS ₂ films in sliding contact in N ₂ gas at different contact stresses. Seven different film compositions were studied. Films with higher metal contents were found to perform especially well at low contact stresses, which is the regime where sliding electrical contacts operate (i.e., <1 MPa). Auger Nanoprobe analysis was used to reveal how low friction is produced, even at contact stresses well below that usually used in MoS ₂ -lubricated systems.					
15. SUBJECT TERMS Solid lubricant films, Molybdenum disulfide, Sliding Electrical contacts, Slip rings, Spacecraft lubrication, Friction and wear testing, Nanocomposite coatings, RF sputter deposition					
16. SECURITY CLASSIFICATION OF:			17. LIMITATION OF ABSTRACT	18. NUMBER OF PAGES	19a. NAME OF RESPONSIBLE PERSON Jeffrey Lince
a. REPORT UNCLASSIFIED	b. ABSTRACT UNCLASSIFIED	c. THIS PAGE UNCLASSIFIED			19b. TELEPHONE NUMBER (include area code) (310)336-4464

Note

The material reproduced in this report originally appeared in *Tribology Letters*. The TR is published to document the work for the corporate record.

Contents

1. Introduction.....	1
2. Experimental method.....	2
3. Results	3
4. Discussion	6
5. Summary	9
Acknowledgments.....	10
References	10

Figures

1. Auger sputter depth profile of a Au/MoS ₂ film, determined by RBS to contain 59 at.% Au.....	3
2. Auger sputter depth profile of a Au/MoS ₂ film, determined by RBS to contain 89 at.% Au.....	4
3. Coefficient of friction traces plotted versus sliding distance for five of the films in this study, obtained at high contact stress.....	4
4. The same data as those shown in figure 1, with the coefficient of friction axis expanded.....	4
5. Coefficient of friction traces plotted versus sliding distance for five of the films in this study, obtained at low contact stress.....	5
6. Scanning electron micrograph of the wear track on a Au/MoS ₂ film with 59% Au, tested at 730 MPa.....	5
7. Auger electron spectra of the unworn and worn areas of the Au/MoS ₂ film with 59% Au, tested at 730 MPa.....	6
8. Auger electron spectra of the unworn and worn areas of the Au/MoS ₂ film with 59% Au, tested at 730 MPa.....	6
9. Auger map of the same region as shown in figure 6, using the S signal	7
10. Auger map of the same region as shown in figure 6, using the Au signal	7

11. Scanning electron micrograph of the wear track on a Au/MoS ₂ film with 59% Au, tested at 0.1 MPa.....	7
12. Auger electron spectra of the unworn and worn areas of the Au/MoS ₂ film with 59% Au, tested at 0.1 MPa.....	8
13. Auger electron spectra of the unworn and worn areas of the Au/MoS ₂ film with 89% Au, tested at 0.1 MPa.....	8
14. Summary of the coefficient of friction and endurance data for the films in this study, obtained at high contact stress.....	9
15. Summary of the coefficient of friction and endurance data for the films in this study, obtained at low contact stress.....	9

1. Introduction

MoS₂-based films have been shown to have superior properties when mixed with small amounts of various metals (generally >10%) during sputter-deposition [1-9] or other ion-based deposition techniques [10]. Such films have been used for a number of years for specialized applications like ball bearings on spacecraft [6-8], and for terrestrial machining applications [9]. MoS₂-based films—sputtered as well as burnished, bonded, and MoS₂/polymer composites—are usually used in the high contact stress regime, i.e., 100–2000 MPa. Below 100 MPa, other types of solid lubricants are often used, including polymers (e.g., PTFE).

The contact stress limitation is driven by the observation that MoS₂, and sputter-deposited MoS₂ specifically, follows the Hertz contact model [11,12], that is, the coefficient of friction (μ) is not constant with load as per Amontons' Law [13], but rather μ is inversely proportional to the Hertzian contact stress. The MoS₂

bulk shear strength is 22 MPa, while that for sputter-deposited MoS₂ films has been measured in the range 25–40 MPa Refs. [11,12], respectively. Based on the model, below 100 MPa, the μ for sputter-deposited MoS₂ would be expected to be prohibitively high: greater than 0.25–0.4.

However, there are low contact stress applications that could benefit from an MoS₂-based thin film lubricant. For example, sliding electrical contacts on space systems, including slip rings, relays, and connectors, must exhibit low contact resistance, with low electrical noise production, while maintaining low torque (i.e., friction) and acceptable wear rates. Unfortunately, lubricating materials used at low contact stress like PTFE and liquid lubricants are generally insulating materials. As such, slip rings for spacecraft use one of two materials systems [14,15]. The first involves precious metal brushes and rings that make sliding contact in the presence of a small amount of oil, but these are limited to lower sliding speeds because of electrical noise caused by hydrodynamic lubricant effects. The second involves silver alloy rings sliding against com-

*E-mail: jeffrey.r.lince@acro.org

posite brush materials that are formed from composites of silver powder and 10–15% of MoS₂ powder (with additions of small amounts of either copper or graphite). Such Ag/MoS₂-based systems can work at a variety of speeds, but the MoS₂ is sensitive to oxidation during manufacture [16,17]. In addition, MoS₂ oxidation can also occur during prelaunch storage and testing in humid atmospheres, resulting in the formation of electrically resistive tarnish (i.e., silver sulfide) on the ring surfaces [15,18]. (The cost of using more noble metals to replace the silver in such composites would be prohibitive.)

The use of nanocomposite films based on a co-sputtered mixture of a noble metal like Au and MoS₂ might not suffer from the limitations of the existing sliding electrical contact materials. Specifically, Au does not tarnish, and resultant films would be thin enough that the cost would not be prohibitive. In addition, it has been demonstrated that co-sputtered metal/MoS₂ films can be used in humid air for extended periods without failure [5,9]. However, there are no data that show they would work at such low contact stresses (e.g., <0.15 MPa or 20 psi for solid lubricated slip ring applications). The metal content would need to be higher than for traditional nanocomposite films to ensure minimal bulk and contact resistance. One goal of the present study is to evaluate such films, specifically co-sputtered Au/MoS₂ films, for low contact stress applications. More generally, we are investigating the influence of metal : MoS₂ ratio on film performance over a wide range of Hertzian contact stresses. We studied films with Au concentrations from 0 to 100%, concentrating on Au contents greater than ~40 at.%. To our knowledge metal concentrations above 55 at.% have not been systematically studied, and no studies of co-sputtered metal/MoS₂ films have been conducted in the very low contact stress regime (i.e., <1 MPa).

2. Experimental method

Hardened 440C steel disks were polished to $R_a \approx 0.03 \mu\text{m}$ roughness, degreased in heptane, and then cleaned in Brulin 815GD detergent (diluted in H₂O), followed by rinsing in distilled H₂O, and drying with nitrogen gas. The samples were then installed into a custom sputter-deposition system. Samples are introduced into a load lock chamber and turbomolecular pumped to a pressure below 1.33×10^{-5} Pa (1×10^{-7} Torr). They are then moved into the main deposition chamber, which is also turbomolecular pumped, and has a base pressure of 1.33×10^{-7} Pa (1×10^{-9} Torr). The system is fitted with three rf-sputtering sources, which can be swiveled, and for this study were pointed toward the center of the substrate table. A Au target and a pressed powder MoS₂ target were installed into two of the sources. The Au source was

operated in a partially unbalanced mode to increase the ion flux on the substrate surface during deposition (the actual ion flux was not measured). Samples were installed at the center of the table, which rotated during deposition to ensure film uniformity. Argon was used as the sputtering gas (99.999% nominal purity), which was passed through an Aeronex Gatekeeper® getter (reduces O₂, H₂O, CO, CH₄, and other impurities to less than 1 ppb) before being introduced into each sputtering source. The gas flow rates were controlled using mass flow transducers. The Ar pressure in the chamber during deposition was generally 4 Pa (3×10^{-3} Torr). The circular targets were 10.2 cm in diameter. The Au and MoS₂ sputtering current densities were each varied between 1 and 2.5 W/cm² to achieve films with varying Au : MoS₂ concentration ratios.

Composition analysis of the films was conducted initially via Auger sputter depth profiling using a PHI 680 Auger Nanoprobe. Ar gas was used as the sputtering gas, and approximate elemental compositions were determined by correcting the Auger electron intensity for each element using correction factors provided by PHI (incorporated into the analysis software). Improved compositions were determined subsequently using Rutherford Backscattering Spectrometry (RBS) at Charles Evans & Associates. RBS uncertainties were 0.5 at.% for Mo and Au, 1 at.% for S, and 5 at.% for C and O. No C or O was detected in any of the films by RBS. The pure MoS₂ film was analyzed via Nuclear Reaction Analysis (NRA), which showed that the carbon content was less than the detection limit of 1 at.%.

Friction/wear testing was conducted in a CSEM Pin-on-Disk Tribometer. The lower specimens (disk) were the Au/MoS₂-coated samples. The upper specimens for the high contact stress tests were uncoated 8 mm 440C steel balls (grade 3, $R_a = 0.01 \mu\text{m}$). The upper specimens for the low contact stress tests were uncoated 6.4 mm 440C steel flats ($R_a \approx 0.03 \mu\text{m}$). Prior to testing, the upper specimens were degreased in heptane, and then cleaned in Brulin 815GD detergent (diluted in H₂O), followed by rinsed in distilled H₂O, and dried with nitrogen gas. For all tests, a 5 N load was used, and the sliding speed was 8 cm/s. Nominal mean Hertzian contact stresses were $S_m \approx 730$ MPa (106,000 psi) for the high contact stress tests, and $S_m \approx 0.1$ MPa (15 psi) for the low contact stress tests. (Nonuniform transfer film formation in the low contact stress tests resulted in contact stresses that were probably 5–10 times higher than the nominal value.) The calibration of the friction force sensor is checked before each test and recalibrated if necessary. It is also checked after each test to ensure that it did not drift during the test. Based on our experience with this procedure, we estimate that the uncertainty in μ is ± 0.001 for a 5 N normal load.

Prior to starting the friction/wear tests, the tribometer enclosure was purged with nitrogen gas (99.999%

nominal purity, passed through an Aeronex Gatekeeper[®] getter, which is advertised to reduce oxygen, water, and other impurities to less than 1 ppb) for greater than one hour, and until the relative humidity was reduced to below 1% RH (measured using a precision hygrometer). The tests were started, and were ended after a 2000 m sliding distance was achieved or when μ rose above 0.5. (The tests were stopped at 2000 m to allow post-test analysis of the upper and lower specimens, and also to ensure that adequate N₂ was present during the test). Tests at both high and low contact stresses were conducted on the same sample, but different radii were chosen for the contact points with the upper specimens to ensure that each test was conducted on virgin film.

3. Results

Auger sputter depth profiling of the Au/MoS₂ films was conducted to determine nominal compositions. The area sputtered was about 1 mm in diameter, and the area analyzed was 150 μ m in diameter. Samples were rotated at 0.5 rpm during sputtering and analysis to give a more uniform sputter crater. Subsequent RBS analysis showed that the compositions determined by Auger were not accurate. For example, sputter depth profiles for two films are shown in figures 1 and 2, indicating Au contents of 38 and 76 at.%, while RBS showed that concentrations were actually 59 at.% Au and 89 at.% Au, respectively. However, the Auger depth profiles provided an important quality control technique while we were optimizing film growth parameters. Figures 1 and 2 indicate that oxygen was present in the Au/MoS₂ films in amounts of at most 2–3 at.%, and that the Au, Mo, and S concentrations are constant to within a few percent throughout the depth of the films.

The friction traces for several of the Au/MoS₂ tests at high contact stress (\sim 730 MPa) are shown in figure 3 (an expanded plot is shown in figure 4). The pure MoS₂ film shows an initially low μ (\sim 0.02) that rises quickly above 100 m sliding distance. The addition of 42 and 59 at.% Au to the MoS₂ films results in significantly improved performance, with μ values that settle near 0.012–0.014 by the end of the 2000 m test. With an increase in the Au content to 75 at.% Au, the initial μ is similar to that of the films with lower Au contents, but begins rising just before half the test is completed, failing soon thereafter. An increase in the Au content to 89 at.% results in a film that fails after only about 30 m. The film with 95% Au and a pure Au film (data not shown) failed after less than 10 m.

A similar plot is shown in figure 5 for the Au/MoS₂ tests at low contact stress (\sim 0.1 MPa). In this case, the pure MoS₂ film shows an initial μ of 0.12, which rises significantly after only 10 m. The films with 42 and 59 at.% Au show μ values of about 0.04, which rise somewhat monotonically throughout the tests. The film with 75 at.% Au also starts at $\mu \sim$ 0.04, but settles near 0.03 by the end of the test. The 89 at.% Au film averages about 0.03 throughout most of the test. The film with 95% Au and the pure Au film failed quickly (i.e., less than one meter; data not shown in figure 5).

Post-test analysis of the worn films on the coated disks was conducted using an Auger Nanoprobe (SEM micrographs could be obtained in the same instrument). Figure 6 shows the wear track on the disk coated with Au(59%)MoS₂, after testing at high contact stress (730 MPa). Areas where Auger spectra were obtained are shown in the photomicrograph. Area 1 is in the unworn region of the film, and Areas 2 through 6 are in the worn (contacting) region of the film. Qualitatively, the appearance of the worn area agrees with a ball-on-plate Hertzian contact region, with greater wear occurring in the center of the wear track (area 5)

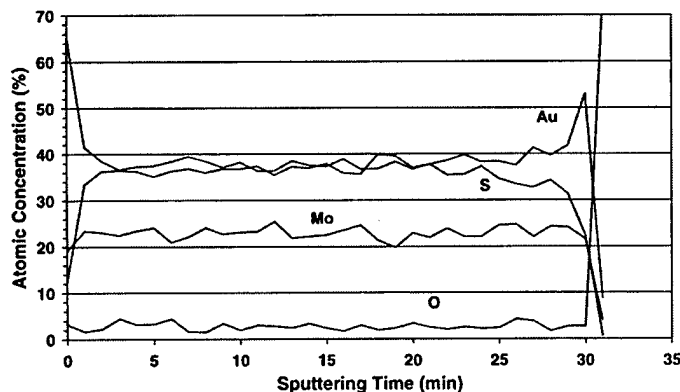


Figure 1. Auger sputter depth profile of a Au/MoS₂ film, determined by RBS to contain 59 at.% Au.

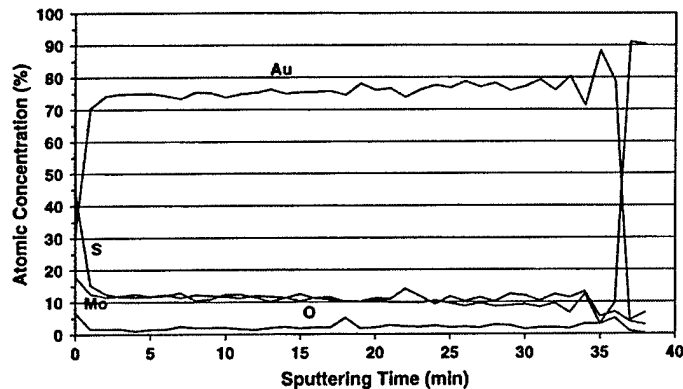


Figure 2. Auger sputter depth profile of a Au/MoS₂ film, determined by RBS to contain 89 at.% Au.

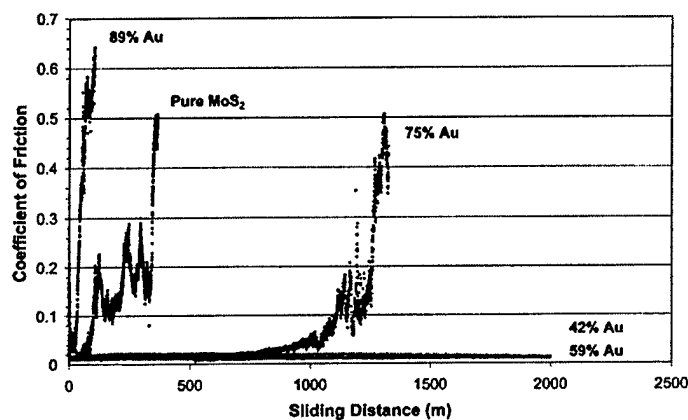


Figure 3. Coefficient of friction traces plotted versus sliding distance for five of the films in this study, obtained at high contact stress ($S_m \sim 730$ MPa, 106 ksi). Data are shown for pure MoS₂, and co-sputtered Au/MoS₂ films with 42, 59, 75, and 89 at.% Au.

than the outskirts of the wear track (area 2), because of the higher contact stress in the center.

Figure 7 shows Auger electron spectra in the unworn (area 1) and worn (area 5) regions of the

Au(59%)/ MoS₂ film shown in figure 6. The film shows the presence of Au, Mo, S, C, and O. The basal plane MoS₂ surface is relatively nonpolar, and therefore shows an affinity for adventitious hydrocarbon

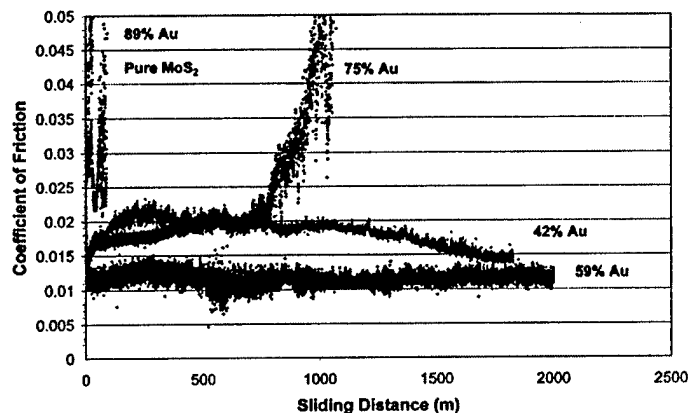


Figure 4. The same data as those shown in figure 1, with the coefficient of friction axis expanded.

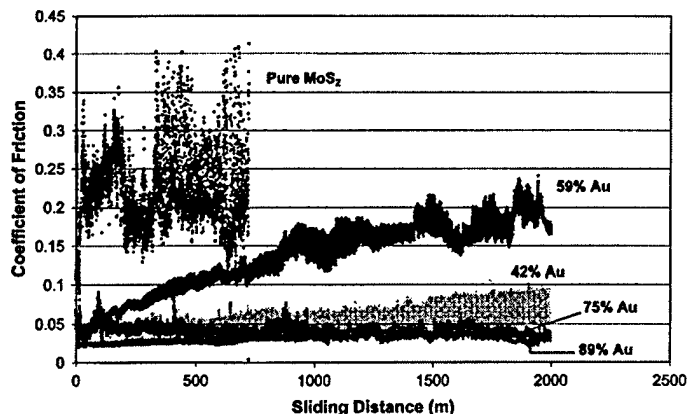


Figure 5. Coefficient of friction traces plotted versus sliding distance for five of the films in this study, obtained at low contact stress ($S_m \sim 0.1$ MPa, 15 psi). Data are shown for pure MoS₂, and co-sputtered Au/MoS₂ films with 42, 59, 75, and 89 at.% Au.

species, so C is always seen on the surface after brief exposures to air. A minimal O peak is seen, since little adsorption of water occurs on this nonpolar surface. It also exhibits very low reactivity, and so little oxidation can occur. The worn surface shows a Au signal that is virtually undetectable. Also, the C and O signals are somewhat higher for the worn surface, because more opportunity for adsorption and oxidation on the film surface occurs during testing, even though high purity nitrogen was used as the ambient atmosphere during testing.

Figure 8 shows the same spectra as in figure 7 for the Au(59%)/MoS₂ film, but the energy axis is expanded to show the high kinetic energy (KE) region. Comparing the spectra for the worn and unworn areas of the film, the Au peaks at higher KE (~ 2000 eV) are not significantly different. This is in contrast to the low KE peak (i.e., at 74 eV), which is visible for the unworn film, and virtually undetectable in the worn area of the film, as discussed above. The inelastic elec-

tron mean free path at 74 eV is ~ 0.4 nm, while at 2000 eV, it is ~ 3 nm [19]. The difference in the high and low KE Au Auger intensities for the worn region indicates that a virtually pure MoS₂ film about a nanometer thick is laying on top of the remainder of the Au-containing film.

Auger electron intensity maps were obtained of the region of the Au(59%)/MoS₂ film shown in figure 6. Figure 9 shows the map for S intensity (representing MoS₂), while figure 10 shows the map for Au intensity (using the 74 eV peak). Within the contact region, the S intensity is significantly higher, while the Au intensity has virtually disappeared. The large drop in Au intensity agrees with the negligible low-KE Au intensity seen in figures 7 and 8 for the worn region.

Figure 11 shows the wear track on the disk coated with Au(59%)/MoS₂, after testing at low contact stress (~ 0.1 MPa). The wear of the film appears more uniform than that for the high contact stress test, because here the contacting upper specimen was flat rather than spherical.

Figure 12 shows Auger electron spectra in the unworn and worn regions of the film shown in figure 11. The spectra appear very similar to the corresponding spectra obtained for high contact stress testing (see figure 8), with the presence of Au, Mo, S, C, and O. As for the high contact stress test, the worn surface shows a significantly smaller Au signal compared to that for the unworn surface.

Figure 13 shows Auger electron spectra in the unworn and worn regions of the disk coated with Au(89%)/MoS₂, after testing at low contact stress (~ 0.1 MPa; corresponding micrograph not shown). The spectrum for the unworn region of the film is similar to those for the Au(59%)/MoS₂ film, (shown in figures 7, 8, and 12), except that the relative height of the Au peaks in the unworn region are much higher. However, the spectrum of the worn region shows a

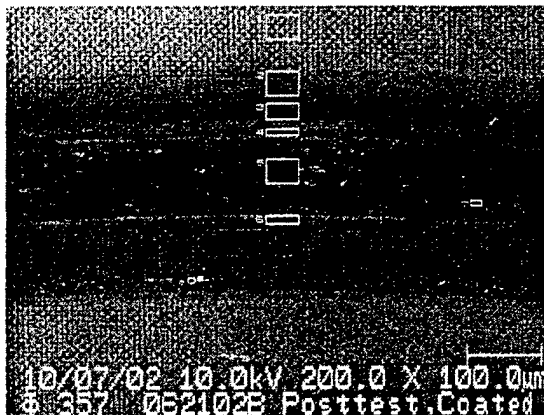


Figure 6. Scanning electron micrograph of the wear track on a Au/MoS₂ film with 59% Au, tested at 730 MPa.

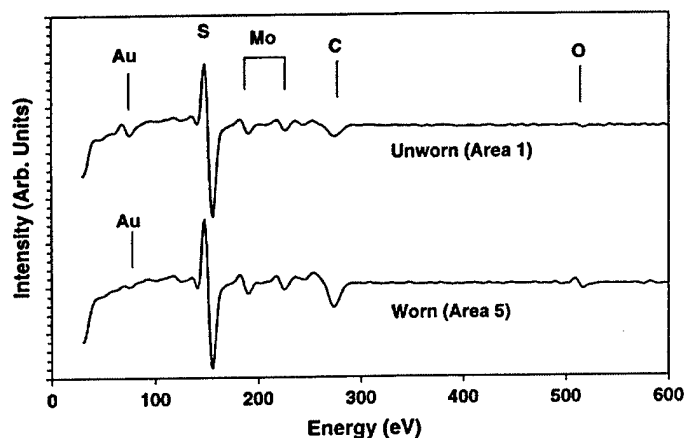


Figure 7. Auger electron spectra of the unworn and worn areas of the Au/MoS₂ film with 59% Au, tested at 730 MPa. These are areas 1 and 5 in figure 6, respectively. Only the low kinetic energy region is shown.

negligibly small Au peak similar in relative intensity to those for the high and low contact stress tests of the Au(59%)/MoS₂ film, even though the bulk Au content in the film is higher.

4. Discussion

Figures 14 and 15 summarize the results of the tribometer testing. The charts show the μ value achieved for each test, which was measured after initial run-in. [For the Au(42%)MoS₂ and Au(59%)MoS₂ films tested at low contact stress, a range of μ values is shown because the μ values continually increased during the tests]. Comparing low and high contact stress results, there are several similarities. Poor performance at both low and high contact stress was seen with the pure MoS₂ film, the pure Au film, and the MoS₂ film with the highest Au content, Au(95%)MoS₂.

For other compositions, however, different composition regimes are optimum for different contact stresses. For high contact stress ($S_m \sim 730$ MPa), the lowest μ and the greatest endurance (within the 2000 m limit of the test) are seen for films with lower Au content: 42 and 59 at.% Au. For low contact stress ($S_m \sim 0.1$ MPa), the films exhibit the lowest μ for films with higher Au content: 75 and 89 at.% Au. Presumably these films would also exhibit the greatest endurance, since the μ values are not increasing at the end of the 2000 m test, in contrast to those with lower Au contents.

There is clearly a difference in the minimum μ values achieved at high versus low contact stress, namely about 0.015 and 0.03, respectively. This could be related to the well documented observation that μ for pure sputtered MoS₂ films increases with decreasing contact stress, as per the Hertzian contact model

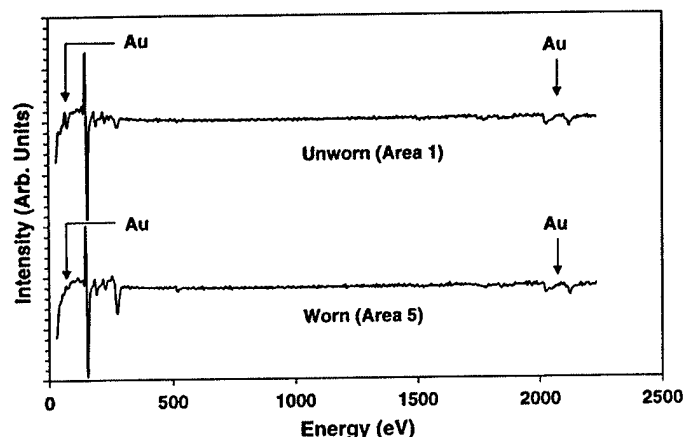


Figure 8. Auger electron spectra of the unworn and worn areas of the Au/MoS₂ film with 59% Au, tested at 730 MPa. These are areas 1 and 5 in figure 6, respectively. Both the low and high kinetic energy regions are shown.

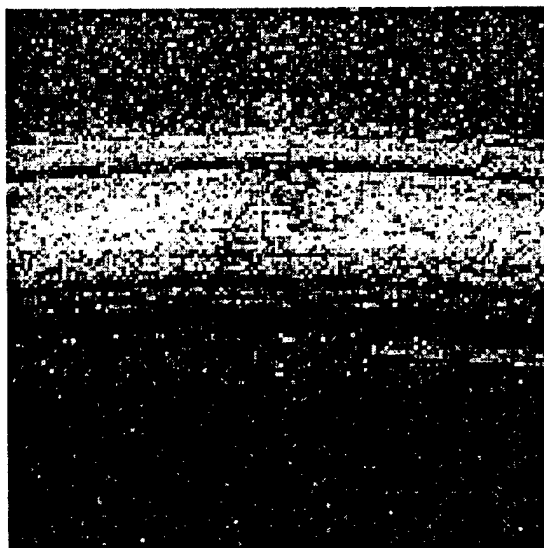


Figure 9. Auger map of the same region as shown in figure 6, using the S signal. Brighter areas indicate a higher S signal.

[11,12]. It is worth attempting to apply the Hertzian contact model to results from the present study. The Au(75%)MoS₂ film is the only one in the present study that exhibited well-defined μ values at both contact stresses, and exhibits μ values of 0.018 and 0.03 at contact stresses estimated at 730 MPa and ~ 1 MPa, respectively (The 1 MPa value is an estimate based on lack of complete area contact for the disk-on-disk test). This gives an approximate shear strength of 83 MPa, which is the same order of magnitude as

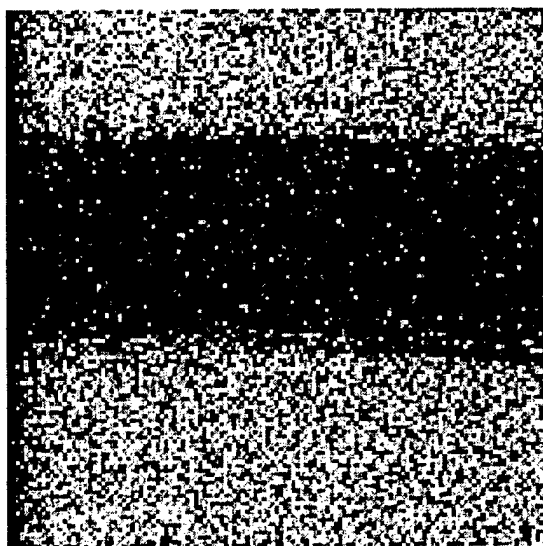


Figure 10. Auger map of the same region as shown in figure 6, using the Au signal. Brighter areas indicate a higher Au signal.

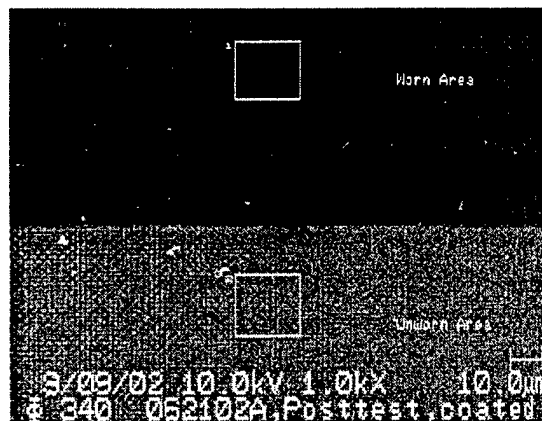


Figure 11. Scanning electron micrograph of the wear track on a Au/MoS₂ film with 59% Au, tested at 0.1 MPa.

obtained previously for pure MoS₂ films, i.e., in the range 25–40 MPa [11,12].

The Auger results reveal that lubrication by Au/MoS₂ films, after run-in, occurs via a virtually pure MoS₂ film that is less than about a nanometer in thickness. This film resides on top of the remainder of the Au/MoS₂ film. This effect has also been seen with other similar metal nanocomposite films: Wahl *et al.* showed that during wear of dual ion-beam-deposited Pb–Mo–S films, the surface of the film was transformed to MoS₂ [20]. In addition, the surface compositions appear highly similar for all films that were studied after 2000 m sliding (i.e., before failure), including after testing at contact stresses that differ by over four orders of magnitude.

Clearly, different film properties are important in different contact stress regimes. Previously, only high contact stress regimes have been extensively studied, and it is generally agreed that co-sputtering metals with MoS₂ produces films with greater density and reduced MoS₂ crystallite size [21,22], resulting in greater hardness [5] and environmental stability [5,9] than pure MoS₂ films. Although the initial μ value for the Au(75%)MoS₂ film tested at 730 MPa is similar to that for films with 42–59 at.% Au, the endurance is significantly lower. This could indicate that the fracture toughness and/or adhesion of the films decrease with increasing Au content. (Preliminary nanoscratch testing results on these films showed that the adhesion did not decrease with increasing Au content, discounting film adhesion as the cause. Results on nanoindentation to obtain hardness and fracture toughness data will be reported in a future publication.) Similar to pure MoS₂ films, pure Au films cannot stand up to high contact stresses, and so fail quickly.

MoS₂-based films are useful as lubricants at high contact stresses – with very thin MoS₂ films providing the lubrication – because the contact stress (730 MPa)

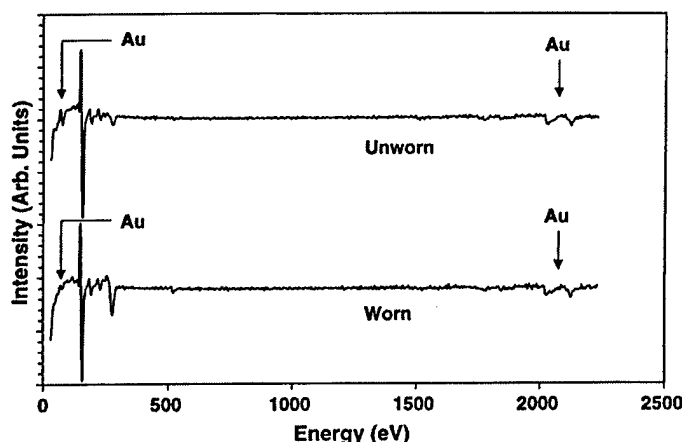


Figure 12. Auger electron spectra of the unworn and worn areas of the Au/MoS₂ film with 59% Au, tested at 0.1 MPa (see figure 11).

is much higher than the shear strength of MoS₂ (25–40 MPa [11,12]). This also results in thin, uniform transfer film formation. An illustration of how variations in transfer film formation affect lubrication performance is a study of the variation in behavior by sputter-deposited MoS₂ films tested in small partial pressures of oxygen or water vapor [23–25]. Specifically, films tested in oxygen (and to a lesser extent vacuum) resulted in thin, uniform transfer film formation, while those tested in water vapor resulted in thick, patchy transfer films, with higher friction and wear rates. These differing behaviors were ascribed to oxygen enhancing the adhesion of the MoS₂ with the opposing surface, probably by forming bridging chemical bonds between the two. Water vapor has a very different effect, enhancing the bonding of MoS₂ particles to each other, probably by surface tension, so that large agglomerations of MoS₂ particles form the transfer films [25], rather than molecularly thin films. The

results of the differing behavior in water vapor and oxygen relate to the present study in that preliminary analysis of the transfer films (i.e., films deposited on the uncoated upper specimen) shows thinner, more uniform transfer for compositions that show the best tribological performance.

In contrast to high contact stresses, low contact stresses ($S_m \sim 0.1$ –1 MPa) do not require Au/MoS₂ films to be fracture tough. However, the contact stresses are considerably lower than the shear strength of MoS₂. As such, typical films with high MoS₂ content have a tendency to form transfer films comprised of larger MoS₂ particles, since the contact stress would not be high enough to shear the particles in the film to give molecularly thin sheets of MoS₂. (This is similar to results from testing pure MoS₂ films in water vapor discussed above.) In contrast, for Au/MoS₂ films with higher Au content, greater amounts of Au result in smaller MoS₂ crystallite sizes [5], so that smaller

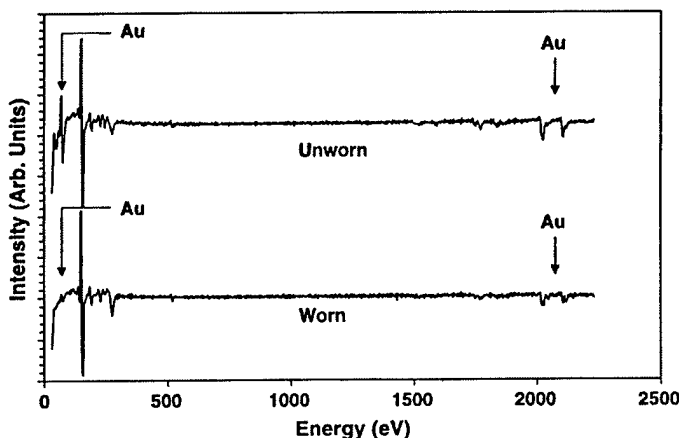


Figure 13. Auger electron spectra of the unworn and worn areas of the Au/MoS₂ film with 89% Au, tested at 0.1 MPa.

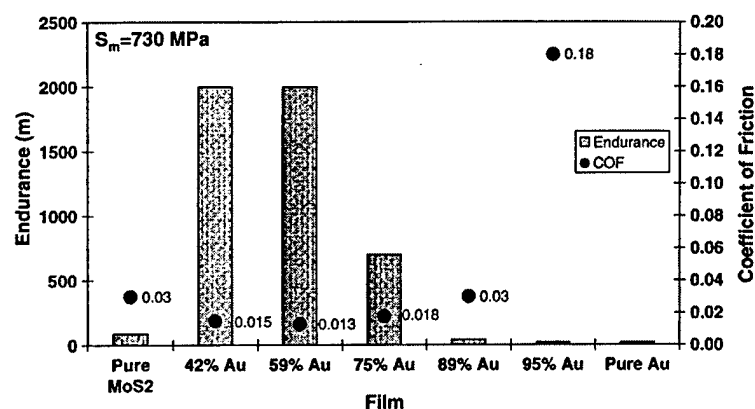


Figure 14. Summary of the coefficient of friction and endurance data for the films in this study, obtained at high contact stress ($S_m \sim 730$ MPa, 106 ksi). Data are shown for pure MoS₂, pure Au, and co-sputtered Au/MoS₂ films with 42, 59, 75, 89, and 95 at.% Au. The μ values were estimated after run-in, and before failure for those films that failed to complete the 2000 m test successfully.

particles are transferred to the opposing surface. In addition, less MoS₂ is available at the surface to form potential transfer films at any moment in time during sliding, so thinner films are transferred. (This is similar to results from testing pure MoS₂ films in oxygen or vacuum discussed above.) However, when the Au content is increased too high, too little MoS₂ is present for adequate lubrication to occur, as indicated by the failure of the Au(95%)MoS₂ film.

These hypotheses of varying behavior of different composition Au/MoS₂ films at different contact stresses will be investigated further during future studies of film nanohardness, adhesion, and transfer film morphology.

Co-sputtered metal/MoS₂ films were previously thought to be useful only at high contact stresses (i.e., ~ 1 GPa). The present study shows that the usefulness of co-sputtered metal/MoS₂ films can be extended to low contact stress regime by increasing the metal

content to an optimum level (we have studied only Au for such applications, but presumably similar behavior could be expected for other metals). Sliding electrical contact technology is a general application area that could benefit from this result, including slip rings, relays, and switches. (Many tribological materials useful at low contact stresses, including polymers like PTFE, are not useful for electrically conducting applications.) The result that higher Au contents give better tribological performance in Au/MoS₂ films also bodes well for electrical contacts, since they would be expected to have higher conductivity as well.

5. Summary

The friction and endurance of nanocomposite, co-sputtered Au/MoS₂ solid lubricant films in sliding contact in N₂ gas was studied at two vastly different

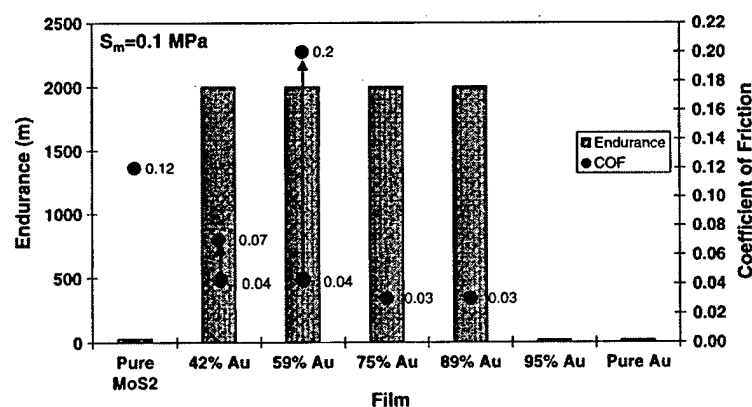


Figure 15. Summary of the coefficient of friction and endurance data for the films in this study, obtained at low contact stress ($S_m \sim 0.1$ MPa, 15 psi). Data are shown for pure MoS₂, pure Au, and co-sputtered Au/MoS₂ films with 42, 59, 75, 89, and 95 at.% Au. The μ values were estimated after run-in, and before failure for those films that failed to complete the 2000 m test successfully.

contact stresses, 730 MPa and ~ 0.1 MPa. Seven different film compositions were studied, with Au contents in the range 42–100 at.%, as well as pure MoS₂. The tests were limited to sliding distances of 2000 m; films lasting that long were considered successful. The results showed that co-sputtered Au/MoS₂ films outperformed both pure sputtered MoS₂ films and pure sputtered Au films. At high contact stresses, the films that performed the best (lowest μ and highest endurance) were films with lower Au contents (i.e., 42 and 59 at.% Au). In contrast, at low contact stress, films with high Au contents (i.e., 75 and 89 at.% Au) performed the best. Films that successfully lasted the 2000 m sliding distance of the test without failure were studied by Auger nanoprobe analysis. Auger spectroscopy revealed that lubrication was provided by a thin film (~ 1 nm thick) of relatively pure MoS₂, regardless of the contact stress. The results suggest possible mechanisms for improved performance with varying composition. For high contact stresses, low Au content provides optimum film properties, while ensuring adequate amounts of MoS₂ remain available at the sliding contact. For low contact stresses, higher Au content limits the amount/size of MoS₂ particles that are transferred to the opposing surface, providing an optimum transfer film for good lubrication. Beyond their interest in explaining solid lubrication phenomena, the results presented here indicate a film composition can be achieved that could be used for low contact stress applications, especially those requiring high electrical conductivity like slip rings.

Acknowledgments

This work was supported under the Aerospace Corporation's Mission Oriented Investigation and Experimentation program, funded by the US Air Force Space and Missile Systems Center under contract no. FA8802-04-C-0001. The author gratefully acknowledges the assistance of Jim Kirsch in the maintenance and operation of the sputter-deposition system.

References

- [1] T. Spalvins, *Thin Solid Films* 118 (1984) 375–384.
- [2] B.C. Stupp, *Thin Solid Films* 84 (1981) 257–266.
- [3] P. Niederhäuser, H.E. Hintermann and M. Maillat, *Proc. Int. Ion Engineering Congress*, Kyoto, Japan, 1983, pp. 1295–1303.
- [4] J.S. Zabinski, M.S. Donley, S.D. Walck, TR Schneider and N.T. McDvitt, *Tribol. Trans.* 38(4) (1995) 894–904.
- [5] M.C. Simmonds, A. Savan, E. Pflüger and H. Van Swygenhoven, *Surf. Coat. Technol.* 126 (2000) 15–24; *J. Vac. Sci. Technol. A* 19(2) (2001) 609–613.
- [6] S.H. Loewenthal, R.G. Chou, G.B. Hopple, W.L. Wenger, *STLE Tribol. Trans.* 37(3) (1994) 505–515.
- [7] E.W. Roberts and W.B. Price, *Proc. Sixth Eur. Space Mechanisms & Tribology Symposium*, Zurich, Switzerland, 4–6 October 1995, pp. 273–278.
- [8] J.R. Lince and P.D. Fleischauer, in: *Space Vehicle Mechanisms: Elements of Successful Design*, ed. P. Conley (Wiley-Interscience, 1998), Chap. 7.
- [9] N.M. Renevier, V.C. Fox, D.G. Teer and J. Hampshire, *Surf. Coat. Technol.* 127 (2000) 24–37.
- [10] K.J. Wahl, L.E. Seitzman, R.N. Bolster, and I.L. Singer, *Surf. Coat. Technol.* 73 (1995) 152–159.
- [11] I.L. Singer, R.N. Bolster, J. Wegand and S. Fayeulle, *Appl. Phys. Lett.* 57(10) (1990) 995–997.
- [12] J.L. Grosseau-Poussard, P. Moine and M. Brendle, *Thin Solid Films* 307 (1997) 163–168.
- [13] G. Amontons, *Memoires de l'Academie Royale des Sciences* (Chez Gerard Kyuper, Amsterdam, 1706), pp. 257–282.
- [14] S.R. Cole and H. Ludwig, Slip-Ring Assemblies, in: *Space Vehicle Mechanisms: Elements of Successful Design*, ed. P. Conley (Wiley-Interscience, 1998), Chap. 15, pt. 1.
- [15] J.R. Lince, Electrical Contact Ring Assemblies, in: *NASA Space Mechanisms Handbook*, ed. R. L. Fusaro (Glenn Research Center, Cleveland, OH, 1999); NASA/TP-1999-206988, Chap. 16.
- [16] J.R. Lince and P.P. Frantz, *Tribol. Lett.* 9(3–4) (2001) 211–218.
- [17] E.W. Glossbrenner and B.K. Witherspoon, Brushes Containing Molybdenum Disulfide for Slip Rings in Spacecraft Application, in *Proceedings of the 33rd IEEE Holm Conference on Electrical Contacts*, Institute of Electrical and Electronics Engineers, New York, 1987, pp. 253–259.
- [18] R. Bauer, *J. Space Craft Rockets* 25(Nov.–Dec. 1988) 439–440.
- [19] C.J. Powell and A. Jablonski, NIST Electron Inelastic-Mean-Free-Path Database, Version 1.1 (National Institute of Standards and Technology, Gaithersburg, MD, 2000).
- [20] K.J. Wahl, D.N. Dunn and I.L. Singer, *Wear* 230(2) (1999) 175–83.
- [21] J.R. Lince, MR Hilton and A.S. Bommanavar, *J. Mater. Res.* 10(8) (1995) 2091–2105.
- [22] M.R. Hilton, G. Jayaram and L.D. Marks, *J. Mater. Res.* 13(4) (1998) 1022–1032.
- [23] P.D. Fleischauer, S.V. Didziulis and J.R. Lince, *Proc. Int. Tribol. Conf.* 2 (2000) 1109–1113.
- [24] P.D. Fleischauer, J.R. Lince and S.V. Didziulis, Chemical Effects on MoS₂ Lubricant Transfer Film Formation; Wear Life Implications, in: *Handbook of Tribology and Lubrication*, Vol. 10, ed. W.J. Bartz (Expert Verlag, 2002), pp. 30–33.
- [25] M.N. Gardos, *Tribol. Lett.* 1 (1995) 67–85.

LABORATORY OPERATIONS

The Aerospace Corporation functions as an "architect-engineer" for national security programs, specializing in advanced military space systems. The Corporation's Laboratory Operations supports the effective and timely development and operation of national security systems through scientific research and the application of advanced technology. Vital to the success of the Corporation is the technical staff's wide-ranging expertise and its ability to stay abreast of new technological developments and program support issues associated with rapidly evolving space systems. Contributing capabilities are provided by these individual organizations:

Electronics and Photonics Laboratory: Microelectronics, VLSI reliability, failure analysis, solid-state device physics, compound semiconductors, radiation effects, infrared and CCD detector devices, data storage and display technologies; lasers and electro-optics, solid-state laser design, micro-optics, optical communications, and fiber-optic sensors; atomic frequency standards, applied laser spectroscopy, laser chemistry, atmospheric propagation and beam control, LIDAR/LADAR remote sensing; solar cell and array testing and evaluation, battery electrochemistry, battery testing and evaluation.

Space Materials Laboratory: Evaluation and characterizations of new materials and processing techniques: metals, alloys, ceramics, polymers, thin films, and composites; development of advanced deposition processes; nondestructive evaluation, component failure analysis and reliability; structural mechanics, fracture mechanics, and stress corrosion; analysis and evaluation of materials at cryogenic and elevated temperatures; launch vehicle fluid mechanics, heat transfer and flight dynamics; aerothermodynamics; chemical and electric propulsion; environmental chemistry; combustion processes; space environment effects on materials, hardening and vulnerability assessment; contamination, thermal and structural control; lubrication and surface phenomena. Microelectromechanical systems (MEMS) for space applications; laser micromachining; laser-surface physical and chemical interactions; micropropulsion; micro- and nanosatellite mission analysis; intelligent microinstruments for monitoring space and launch system environments.

Space Science Applications Laboratory: Magnetospheric, auroral and cosmic-ray physics, wave-particle interactions, magnetospheric plasma waves; atmospheric and ionospheric physics, density and composition of the upper atmosphere, remote sensing using atmospheric radiation; solar physics, infrared astronomy, infrared signature analysis; infrared surveillance, imaging and remote sensing; multispectral and hyperspectral sensor development; data analysis and algorithm development; applications of multispectral and hyperspectral imagery to defense, civil space, commercial, and environmental missions; effects of solar activity, magnetic storms and nuclear explosions on the Earth's atmosphere, ionosphere and magnetosphere; effects of electromagnetic and particulate radiations on space systems; space instrumentation, design, fabrication and test; environmental chemistry, trace detection; atmospheric chemical reactions, atmospheric optics, light scattering, state-specific chemical reactions, and radiative signatures of missile plumes.